Nanofluidic ions transport and energy conversion through ultrathin free-standing polymeric carbon nitride membranes.

Kai Xiao, Paolo Giusto, Liping Wen, Lei Jiang and Markus Antonietti

An ultrathin free-standing polymeric carbon nitride membrane (UFSCNM) is
fabricated by simple CVD polymerization and exhibits excellent surface-charge-
governed ion transport properties, which endow UFSCNM with function of salinity
gradient energy conversion. With advantage of low cost, facile fabrication, and ease of
scaling up to support high ionic currents, UFSCNM should be an alternative for new
ionic device designs.

Nanofluidic ions transport and energy conversion through ultrathin free-standing polymeric carbon nitride membranes

Kai Xiao*, Paolo Giusto, Liping Wen, Lei Jiang and Markus Antonietti*

Abstract: Ions transport through confined space with characteristic dimensions comparable to the Debye length has many applications, e.g. in water desalination, dialysis, and energy conversion. However, the existing 2D/3D smart porous membrane for ions transport and further applications are always fragile, thermolabile, and/or difficult to scale up, limiting their practical applicability. Here, we report that polymeric carbon nitride alternatively allows creating an ultrathin free-standing carbon nitride membrane (UFSCNM), which can be fabricated by simple CVD polymerization and exhibits per se excellent nanofluidic ions transport properties. The surface-charge-governed ion transport also endows such UFSCNMs with the function of converting salinity gradients into electric energy. With advantages of low cost, facile fabrication, and the ease of scale up while supporting high ionic currents, UFSCNM can be considered as an alternative candidate for the energy conversion system and new ionic devices.

Ion transport is a ubiquitous phenomenon in cellular membranes and is also crucial for life's essential functions.[1] To mimic and better understand the functions of ion transport system, solid-state nanofluidic system were proposed.[2] In the confined nanofluidic nanochannel, nanotube, and nanopore with a characteristic size typically on the order of 1-100 nm, the ion transport always exhibits significantly differences to the bulk, and includes emerging effects as ion selectivity, ion rectification, and ion gating properties.[3] These unique characters can be utilized in many fields, for example water desalination, dialysis, and ion filtration. In salinity gradient energy conversion as an example,[4] the dimensions of the channels are close to the Debye screening length, and the surface charge of the channels can drastically alter the ionic behaviors of the nanofluids. This effectively repels the counter ions, allowing only the target ions to transport through. To realize the large-scale harvesting of salinity gradient energy, it is however necessary to develop new avenues and low-cost membranes which are mechanically, chemically, and thermally more robust, while possessing a higher permeability and selectivity at the same time.[5]

Two-dimensional materials,[6] for example graphene and graphene oxide (GO), would represent the ultimate step for such membranes, and nanosheets with similar 2D structures have been assembled into nano-channeled membranes, a hot topic of scientific research.[7] For instance, Huang et.al realized the ion transport nanofluidic based on reconstructed layered graphene oxide paper.[8] Recently, Geim et.al described the ions transportation properties through angstrom-scale graphene slits.[9] These nanosheet membranes already have demonstrated the desired advantages, such as outstanding separation performance, flexibility, and interesting nanoscale fluidics properties.[6] Two dimensional carbon nitride (C_3N_4) materials are another obvious choice with inherent lateral porosity, and it already attracted broad interest with its broad applications in sensing, bio-imaging, novel solar energy exploitation, as well as photocatalysis.[10] Meanwhile, membrane materials and methods based on carbon nitride have been developed to realize water transport,[11] actuators,[12] and separation,[13] all questions closely related to the current work. However, the ion transport properties through the 2D layered polymeric carbon nitride membrane has to our knowledge never been explored. With advantages of low cost, facile fabrication, and the ease of scale up, the 2D carbon nitride materials provide a possibility for engineered new ionic devices.

Here, we demonstrate the realization of a 2D ultrathin free standing polymeric carbon nitride membrane (UFSCNM) which can be used for manipulation of ions transportation and salinity gradient energy conversion because of its unique layered structure. The fabrication process is realized by vapor-deposition polymerization (VDP) or chemical vapor deposition (CVD) and is illustrated in **Figure 1a, b.** In general, the UFSCNM is synthesized by polymerization of appropriate starting materials, such as melamine or Gdm_2CO_3. After thermal polymerization in the test tube, a yellowish transparent membrane is formed on the glass surface, in coexistence with a yellowish carbon nitride power in the tube. The UFSCNM can be easily delaminated from the glass substrate without damage by soaking with water, already indicating its porosity.

Figure 1c showed the optical and the enlarged SEM images of a UFSCNM. At the macroscopic level, the UFSCNM is transparent; and micrococscopically, the UFSCNM is smooth and has no obvious defects, a mandatory requirement for the desired membrane applications. This suggests that the ions can only transport though the crack-free membrane by the inherent carbon nitride pores, supported by the interlayer spacings. The highly oriented layer structure parallel to the surface can be clearly confirmed by the scanning electron microscopy (SEM) and transmission electron microscopy (TEM) images (**Figure 1d, e, s1**). X-ray diffraction (XRD) of the carbon nitride power and UFSCNM revealed the peak corresponding to the (002) plane of the layered structure (**Figure 1f**).[12, 14] All these results confirmed the 2D graphitic carbon nitride structure of UFSCNM. Meanwhile, the UFSCNM is not isotropic in the plane and has some specific orientations enhanced in the structure. High-resolution TEM and electron diffraction images also showed the crystalline membrane structure (**Figure 1g**). In addition, X-ray photoelectron spectroscopy (XPS) showed two typical C 1s peaks at 284.8 and 288.1 eV that can be assigned to the sp^2 C in carbonaceous environment and sp^2 C in C-N heterocycles, respectively (**Figure s2**). The N 1s spectra can be deconvoluted into three peaks,

[*]   Dr. K. Xiao, P. Giusto, Prof. Dr. Markus Antonietti
        Max Planck Institute of Colloids and Interfaces, Department of
        Colloid Chemistry, D-14476 Potsdam, Germany.
        E-mail: xiaokai@iccas.ac.cn; Markus.Antonietti@mpikg.mpg.de
        Prof. L. Wen, Prof. L. Jiang
        Key Laboratory of Bio-inspired Materials and Interfacial Science
        Technical Institute of Physics and Chemistry, Chinese Academy of
        Sciences, Beijing 100190, P.R. China.

        Supporting information for this article is given via a link at the end of
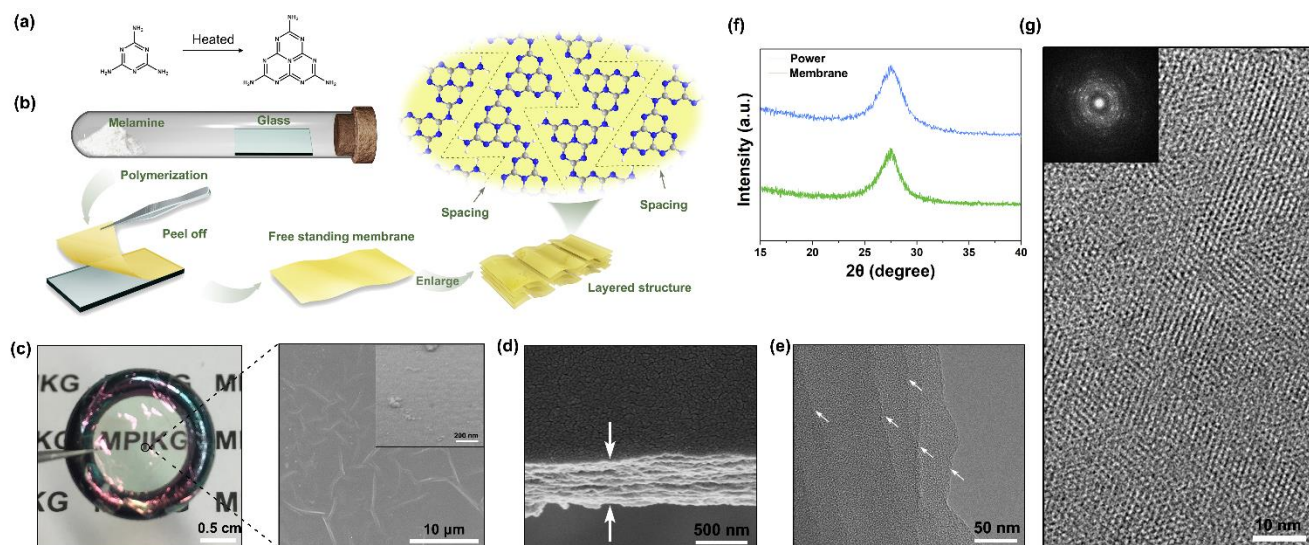   the document.

Figure 1. a) The synthetic route of UFSCNM. b) Schematic illustration of the vapour-deposition polymerization fabrication process and the molecular structure of UFSCNM. c) Optical and the enlarged SEM images of a UFSCNM peeled off a glass substrate after CVD. d) The cross section of the multi-layered-UFSCNM. e) The TEM image of layered structure, white arrows: layered edge. f) The XRD of carbon nitride power and UFSCNM. g) The high-resolution TEM and electron diffraction indicated the UFSCNM was crystallized.
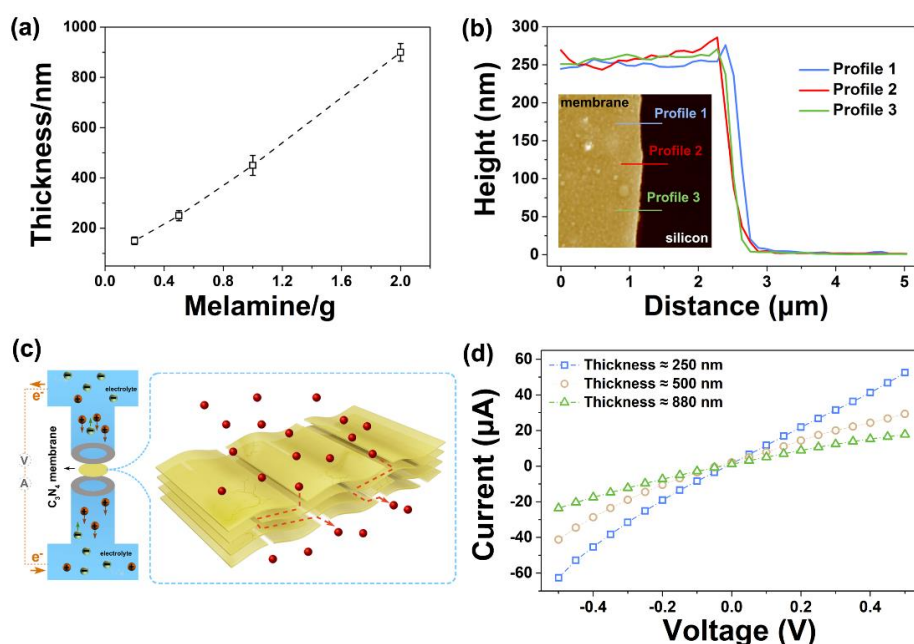

Figure 2. a) The thickness of UFSCNM as a function of melamine. b) Typical AFM height images of the section of an as-pre`pared UFSCNMs transferred onto silicon wafer and the corresponding height profile with thickness about 250 nm. c) Schematic of ions transport across the UFSCNMs. d) The current-voltage curves of the UFSCNMs with thickness 250 nm, 500 nm, and 880 nm.

In this work, the thickness of UFSCNM was well controlled by changing the amount of melamine, in the range from about 140 nm to 1 µm (**Figure 2a and s4**). This can be imaged using atomic force microscopy (AFM) by freeze-cracking the UFSCNM and then putting the fragments onto a silicon wafer. **Figure 2b** showed the typical AFM image of an as-prepared UFSCNM with thickness about 250 nm. Thinner membranes could in principle be made, but turned out to be difficult to be delaminated from the glass substrate without damage. Of course it is the ultimate goal to use few layer carbon nitride structure, but this has to await more professional deposition conditions.

The membranes with thickness of approximately 250 nm, 500 nm, and 880 nm were also used to study the ions transportation properties, which were measured by using the Ag/AgCl electrodes to characterize the current-voltage (*I-V*) curves across the membrane in 1 mM KCl electrolyte (**Figure 2c**). **Figure 2d** showed the corresponding *I-V* characteristics of UFSCNMs with thickness 250 nm, 500 nm, and 880 nm, respectively. The ionic current under 0.5 V decreased from about 60 µA to 20 µA along with the increase of membrane thickness, which can be ascribed to the corresponding increasing resistance and also points to the defect pores, homogeneous structure of the membranes.
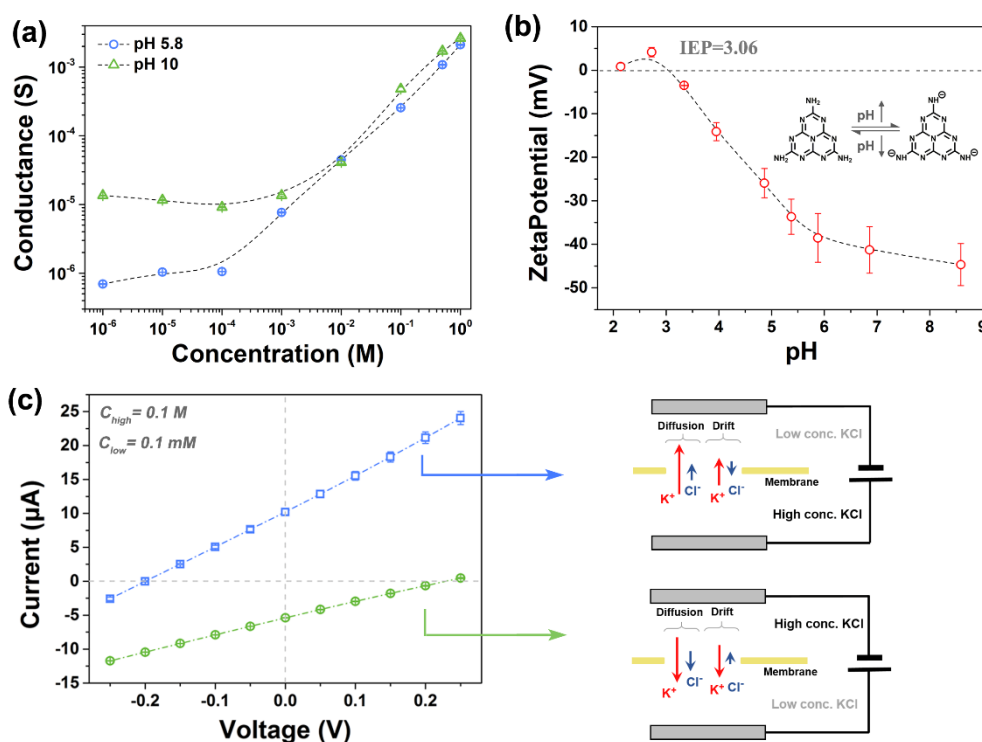
398.6 eV (C=N-C), 399.9 eV (N-C$_3$), and 400.9 eV (C-NH-C and C-NH$_2$), consistent with previous work.[14] Meanwhile, the UFSCNM possess residues of unreacted amino and imino groups (**Figure s3**), mainly along the edges of their 2D structure, which represents a crucial factor to regulate the charge density and control the ions transportation.

Figure 3. a) Conductance as a function of salt concentration at pH 5.8, and pH 10, indicating the surface charge controlled ion transportation. b) Zeta potential of UFSCNM as a function of pH, the IEP was estimated to be about 3.06. The inset shows the pH-responsive surface properties. c) Measures *I-V* curves for two different salt concentration gradient configurations and the schematic of diffusion current, indicating the ion selectivity of the UFSCNMs.

consistent with the net flow of positive charges from high to low concentration, which also immediately indicates that the pore is ion selective.[17] As shown in **Figure 3c**, in the absence of external voltage (V=0), both the cation (K^+) and anion (Cl^-) diffuse from high concentration (0.1 M) to low concentration (0.1 mM), and a net current (short-circuit current I_{SC}) is observed only if one ion diffuses at a higher rate than the other through the pore. The direction of I_{SC} is consistent with the net flow of positive charges from high to low concentration. In consequence, the reverse of the concentration gradient configuration results into the reverse of I_{SC}. The ion selectivity is important for the creation of electric energy from salinity gradients, because it has been proven that the potential and current stem only from the charge separation.[3b, 18]

To confirm that confinement effects as well as surface charge control ion transportation properties, we measured the ionic conductivity of UFSCNM system as a function of KCl concentration and pH. In general, the conductivity of bulk KCl solution is proportional to its concentration.[8, 15] For the UFSCNM system, at high salt concentration, ionic transport through UFSCNM is similar to that of the bulk electrolyte solution. However, this conductivity begins to deviate from bulk behavior at ~10^{-3} M and gradually plateaus at lower concentrations for pH 5.8 and 10 (**Figure 3a**). This is the signature of surface charge controlled ions transportation properties.[16] At both pH 5.8 and 10, the UFSCNM is negative charged because of the incomplete polymerization or condensation with electron rich -NH terminal group (**Figure 3b**), therefore conductivity becomes independent of the nominal ionic concentrations because of the cation selectivity at low concentrations.

To further confirm the ion selectivity behavior of the charged UFSCNM, we investigated two different configurations of salt concentration gradients (C_{high}/C_{low}=1000) across the UFSCNM at pH 6.8. The direction of the short-circuit current is

The electroosmotic potential and current were measured with a variety of KCl concentration gradients across the membrane with a thickness 250 nm to further test the potential of power generation. The energy conversion performance can be directly calculated from the intercepts on the current axe (I_{SC}) and voltage axe (open-circuit voltage: V_{OC}). As shown in **Figure 4a**, both the I_{SC} and V_{OC} scale inversely with the thickness of UFSCNMs. In fact, the measured V_{OC} consists of two parts: the diffusion potential (E_{diff}) which is contributed by the power source, and the redox potential (E_{redox}) which is generated by the non-equal potential drop at the electrode-solution interfaces.[4b, 19] The redox potential (E_{redox}) follows the Nernst
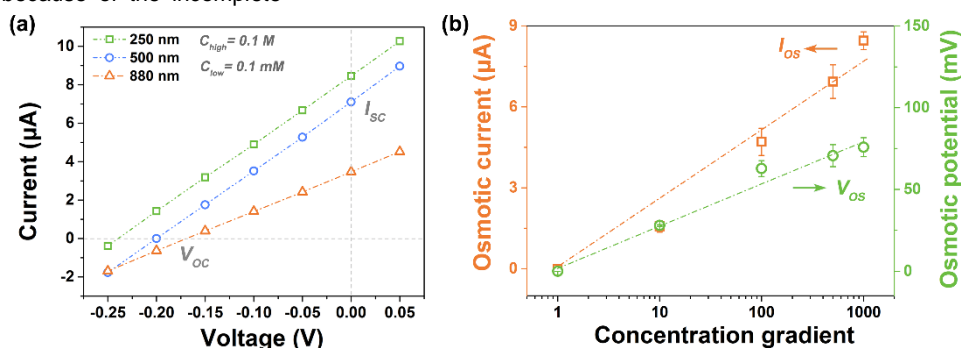

Figure 4. a) Electroosmotic power generation for UFSCNMs with thickness 250 nm, 500 nm, and 880 nm under salt concentration gradient 1000 (C_{high}/C_{low} = 0.1 M/0.1 mM). b) The pure osmotic potential V_{OS} and current I_{OS} as a function of salt gradient for the 250 nm thickness UFSCNM.

equation (**Figure s7, s8 and table s1**), and its contribution at different concentrations were subtracted to estimate the pure electroosmotic potential (V_{OS}) and electroosmotic current (I_{OS}). As shown in **Figure 4b**, the V_{OS} increased from about 28 mV to 76 mV while the I_{OS} increased from 1.6 μA to 8.5 μA along with the increase of salt concentration gradient from 10-fold to 1000-fold. Calculated by the equation: $P_{max}=E_{diff}^2/4r= V_{OS}^2/4r$ (r is the reciprocal of conductance),[19b, 20] the maximum output power of the energy harvesting system can be estimated as 0.21 W/m^2 for 1000-fold salt concentration gradient. This power density is consistent with other 2D materials in salinity gradient energy conversion system.[21] Nevertheless, there is much room to further improve the power density by controlling surface charge density by chemical modifications, while the ion flux can also be optimized by thinner, then more perfect UFSCNMs.

In summary, we generated free standing, practically crack-free polymeric carbon nitride membranes with some hundred nanometer thickness and showed that those structures allow controlled water and ion transport, potentially to the inherent porosity of the materials as such. The membranes were used for manipulation of ion transport and salinity gradient energy conversion. Even in spite of the low power density of 0.21 W/m^2, the approach is due to its simplicity interesting as such, and a potential perfected carbon nitride 2 nm oligolayer, then possibly grown by atomic layer deposition (ALD)-like processes on a support, would result in 100 times higher fluxes. We understand the current ultrathin free standing polymeric carbon nitride however already now as an ideal candidate to analyze question of chemical ion selectivity, the role of possible polymorph control and chemical functionalization on the ion transport as well as all other practical applications which benefit from the advantage of a low-cost, thermally and mechanically robust, and simple fabrication process.

[1] a) E. Gouaux, R. MacKinnon, *Science* **2005**, *310*, 1461-1465; b) B. Hille, *Ion channels of excitable membranes, Vol. 507*, Sinauer Sunderland, MA, **2001**.

[2] C. R. Martin, Z. S. Siwy, *Science* **2007**, *317*, 331-332.

[3] a) K. Xiao, L. Wen, L. Jiang, *Small* **2016**, *12*, 2810-2831; b) H. Daiguji, *Chem. Soc. Rev.* **2010**, *39*, 901-911; c) W. Sparreboom, A. van den Berg, J. C. Eijkel, *Nat. Nanotechnol* **2009**, *4*, 713-720.

[4] a) Z. Zhang, X. Sui, P. Li, G. Xie, X.-Y. Kong, K. Xiao, L. Gao, L. Wen, L. Jiang, *J. Am. Chem. Soc.* **2017**, *139*, 8905-8914; b) J. Feng, M. Graf, K. Liu, D. Ovchinnikov, D. Dumcenco, M. Heiranian, V. Nandigana, N. R. Aluru, A. Kis, A. Radenovic, *Nature* **2016**, *536*, 197-200.

[5] a) H. B. Park, J. Kamcev, L. M. Robeson, M. Elimelech, B. D. Freeman, *Science* **2017**, *356*, eaab0530; b) Z. Zhang, L. Wen, L. Jiang, *Chem. Soc. Rev.* **2018**, *47*, 322-356 .

[6] J. J. Shao, K. Raidongia, A. R. Koltonow, J. Huang, *Nat. Commun.* **2015**, *6*, 7602.

[7] J. Gao, Y. Feng, W. Guo, L. Jiang, *Chem. Soc. Rev.* **2017**, *46*, 5400-5424.

[8] K. Raidongia, J. Huang, *J. Am. Chem. Soc.* **2012**, *134*, 16528-16531.

[9] A. Esfandiar, B. Radha, F. Wang, Q. Yang, S. Hu, S. Garaj, R. Nair, A. Geim, K. Gopinadhan, *Science* **2017**, *358*, 511-513.

[10] a) J. Liu, H. Wang, M. Antonietti, *Chem. Soc. Rev.* **2016**, *45*, 2308-2326; b) F. K. Kessler, Y. Zheng, D. Schwarz, C. Merschjann, W. Schnick, X. Wang, M. J. Bojdys, *Nat. Rev. Mater.* **2017**, *2*, 17030.

[11] Y. Wang, L. Li, Y. Wei, J. Xue, H. Chen, L. Ding, J. Caro, H. Wang, *Angew. Chem. Int. Ed.* **2017**, *56*, 8974-8980.

[12] H. Arazoe, D. Miyajima, K. Akaike, F. Araoka, E. Sato, T. Hikima, M. Kawamoto, T. Aida, *Nat. Mater.* **2016**, *15*, 1084-1089.

[13] X. Wang, G. Wang, S. Chen, X. Fan, X. Quan, H. Yu, *J. Membrane Sci.* **2017**, *541*, 153-161.

[14] L. Lin, H. Ou, Y. Zhang, X. Wang, *ACS Catalysis* **2016**, *6*, 3921-3931.

[15] D. Stein, M. Kruithof, C. Dekker, *Phys. Rev. Lett.* **2004**, *93*, 035901.

[16] a) K. Xiao, G. Xie, Z. Zhang, X.-Y. Kong, Q. Liu, P. Li, L. Wen, L. Jiang, *Adv. Mater.* **2016**, *28*, 3345-3350; b) X. Li, T. Zhai, P. Gao, H. Cheng, R. Hou, X. Lou, F. Xia, *Nat. Commun.* **2018**, *9*, 40.

[17] R. C. Rollings, A. T. Kuan, J. A. Golovchenko, *Nat. Commun.* **2016**, *7*, 11408.

[18] a) L. Cao, W. Guo, W. Ma, L. Wang, F. Xia, S. Wang, Y. Wang, L. Jiang, D. Zhu, *Energ. Environ. Sci.* **2011**, *4*, 2259; b) H. Daiguji, Y. Oka, K. Shirono, *Nano Lett.* **2005**, *5*, 2274-2280.

[19] a) J. Gao, W. Guo, D. Feng, H. Wang, D. Zhao, L. Jiang, *J. Am. Chem. Soc.* **2014**, *136*, 12265-12272; b) D. K. Kim, C. H. Duan, Y. F. Chen, A. Majumdar, *Microfluidi. Nanofluid.* **2010**, *9*, 1215-1224; c) T. B. H. Schroeder, A. Guha, A. Lamoureux, G. VanRenterghem, D. Sept, M. Shtein, J. Yang, M. Mayer, *Nature* **2017**, *552*, 214-218.

[20] W. Ouyang, W. Wang, H. Zhang, W. Wu, Z. Li, *Nanotechnology* **2013**, *24*, 345401.

[21] a) J. Ji, Q. Kang, Y. Zhou, Y. Feng, X. Chen, J. Yuan, W. Guo, Y. Wei, L. Jiang, *Adv. Funct. Mater.* **2017**, *2*, 1603623; b) S. Qin, D. Liu, G. Wang, D. Portehault, C. J. Garvey, Y. Gogotsi, W. Lei, Y. Chen, *J. Am. Chem. Soc.* **2017**, *139*, 6314-6320.